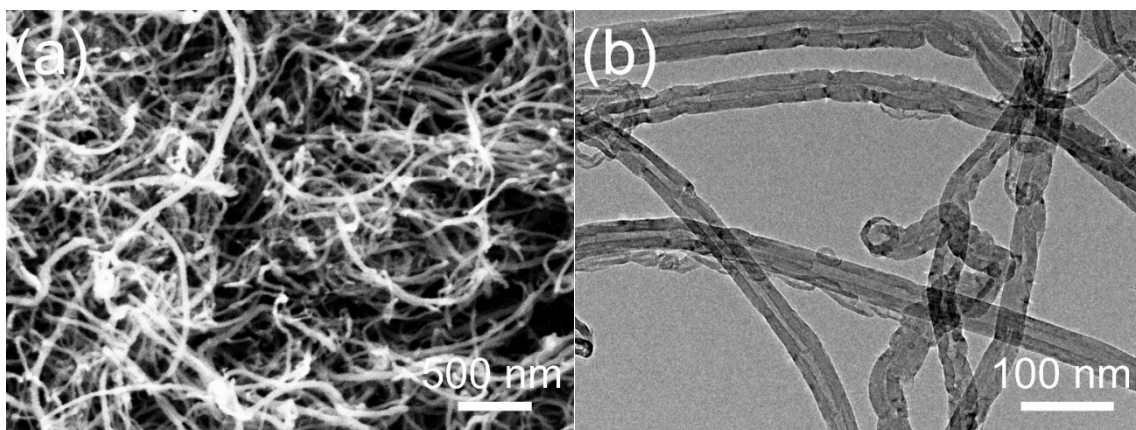


**Supporting Information for**  
**Superior rate-capability and long-lifespan carbon nanotube-in-nanotube@Sb<sub>2</sub>S<sub>3</sub>**  
**anode for lithium-ion storage**

Z.Y. Yang,<sup>a</sup> Y.F. Yuan\*,<sup>a</sup> M. Zhu,<sup>a</sup> S.M. Yin,<sup>a</sup> J. P. Cheng<sup>b</sup> and S.Y. Guo<sup>a</sup>

<sup>a</sup>College of Machinery and Automation, Zhejiang Sci-Tech University, Hangzhou 310018, China

<sup>b</sup>School of Physics and Microelectronics, Zhengzhou University, Zhengzhou 450052, China



**Figure S1** (a) SEM and (b) TEM images of CNTs.

---

\* Corresponding author. *E*-mail address: [yuanyf@zstu.edu.cn](mailto:yuanyf@zstu.edu.cn) (Y.F. Yuan)

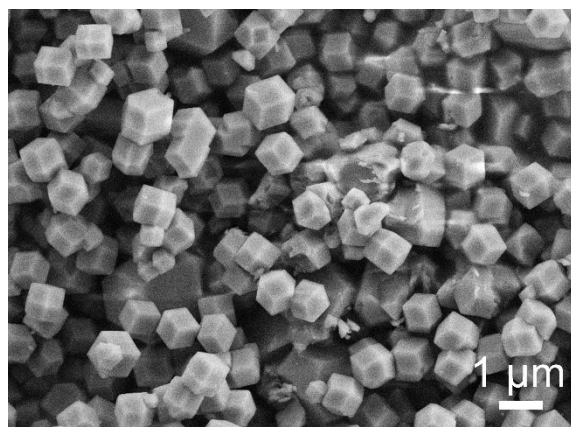


**Figure S2** ZIF-8 polyhedra particles synthesized without the addition of CNTs.

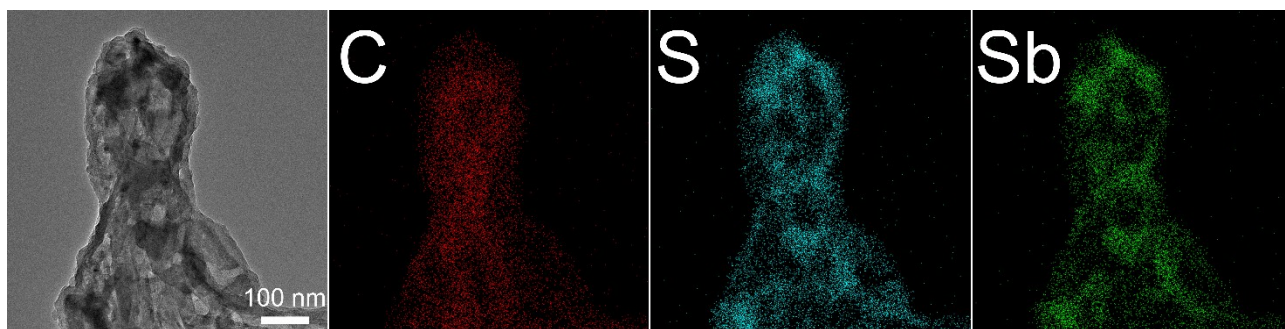


**Figure S3** TEM image of the CNN@Sb<sub>2</sub>S<sub>3</sub> composite and the corresponding EDS mapping of the C, S and Sb elements.

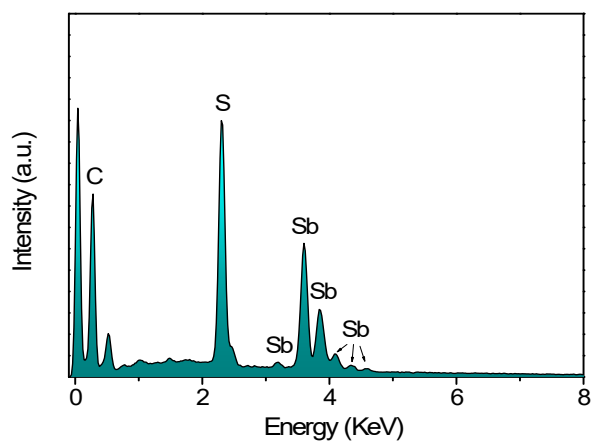


**Figure S4** EDS spectrum of CNN@Sb<sub>2</sub>S<sub>3</sub>.

## Calculation of weight percentages of $\text{Sb}_2\text{S}_3$ , Sb and carbon in the composite

- EDS spectrum indicates that the atomic contents of Sb and S are 5.56% and 7.31%. Therefore, the atomic ratio of Sb and S is 1:1.3.

- S is 7.31%. This means that Sb in  $\text{Sb}_2\text{S}_3$  is 4.87% ( $7.31\%/3 \times 2$ ). Thus, the metallic Sb is 0.69% ( $5.56\%-4.87\%$ ).

The molar ratio of  $\text{Sb}_2\text{S}_3$  : Sb = 2.44 : 0.69

The weight ratio of  $\text{Sb}_2\text{S}_3$  : Sb = 9.85 : 1

- TGA indicates that at 720 °C, the residual matter is  $\text{Sb}_2\text{O}_3$  and its weight stabilizes at 54.96%.

$\text{Sb}_2\text{O}_3$  comes from oxidation of  $\text{Sb}_2\text{S}_3$  and Sb.

In the composite, the weight of Sb is set as x%. Then, the weight of  $\text{Sb}_2\text{S}_3$  is 9.85x%.

$$9.85x \times 291.5/339.7 + x \times 291.5/243.4 = 54.96$$

$$x = 5.7$$

$$\text{Sb}(\text{wt}\%) = 5.7\%, \text{Sb}_2\text{S}_3(\text{wt}\%) = 56.1\%$$

$$\text{C}(\text{wt}\%) = 100\% - 56.1\% - 5.7\% - 1.6\%(\text{water}) = 36.6\%$$

$$\text{After water is deducted, Sb}(\text{wt}\%) = 5.8\%, \text{Sb}_2\text{S}_3(\text{wt}\%) = 57\%, \text{C}(\text{wt}\%) = 37.2\%$$

- The theoretical capacities of  $\text{Sb}_2\text{S}_3$ , Sb and carbon are 947, 660 and 372 mAh  $\text{g}^{-1}$ .

$$\text{The theoretical capacity of the composite} = 947 \times 0.57 + 660 \times 0.058 + 372 \times 0.372$$

$$= 716.5 \text{ mAh g}^{-1}$$

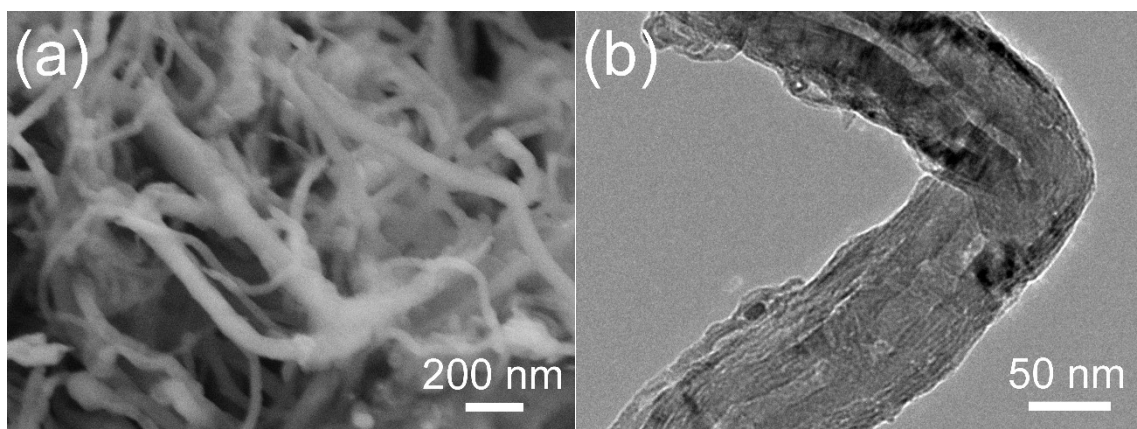


**Figure S5** (a) SEM and (b) TEM images of CNTs@C as the control material.

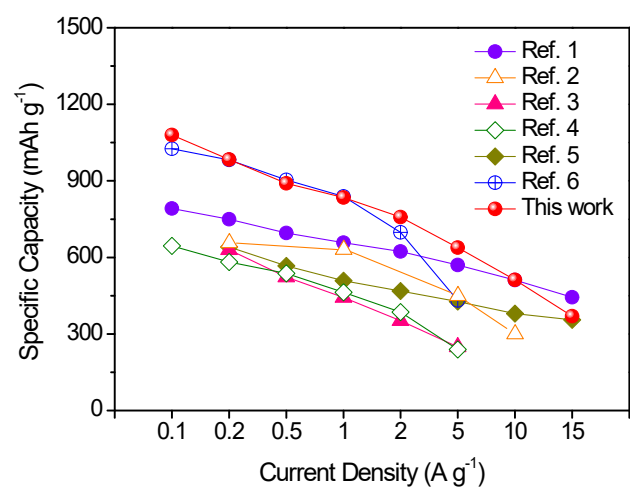


**Figure S6** Comparison of rate capability between CNN@Sb<sub>2</sub>S<sub>3</sub> and previously reported Sb<sub>2</sub>S<sub>3</sub>-based composites.

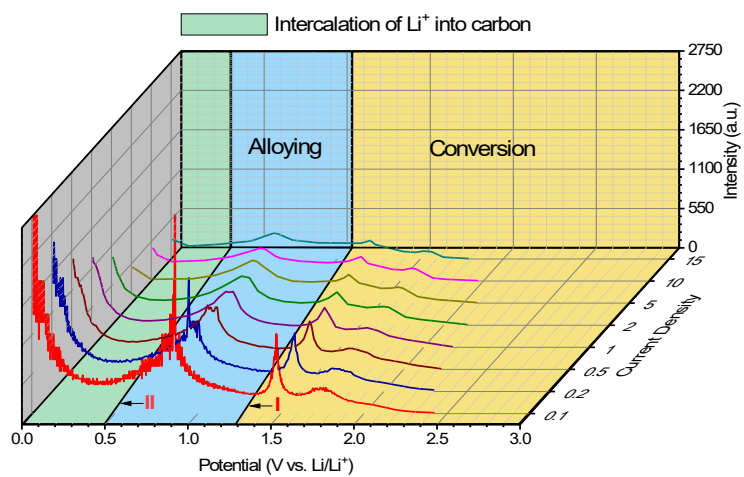


**Figure S7**  $dQ/dV$  curves of rate discharge profiles of  $\text{CNN@Sb}_2\text{S}_3$ .



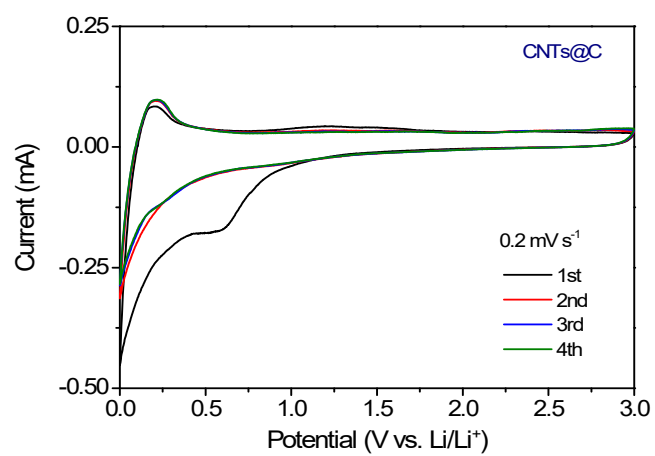


**Figure S8** CV curves of CNTs@C in the first four cycles at a scan rate of 0.2 mV s<sup>-1</sup>.

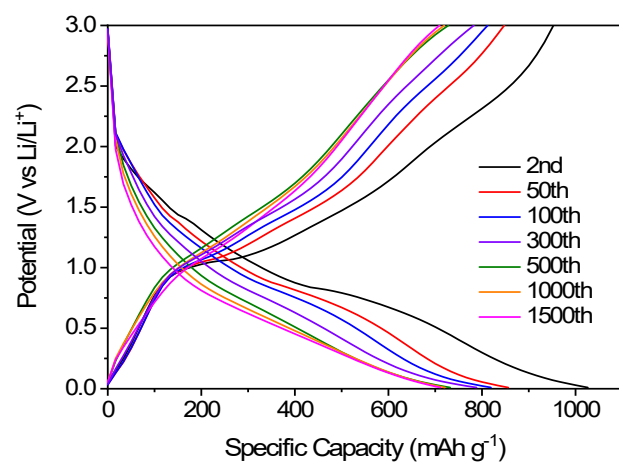


**Figure S9** Galvanostatic discharge and charge curves of CNN@Sb<sub>2</sub>S<sub>3</sub> at the different cycles at the current density of 1 A g<sup>-1</sup>.

**Table S1** Cycling performance comparison between CNN@Sb<sub>2</sub>S<sub>3</sub> and previously reported Sb<sub>2</sub>S<sub>3</sub>-based composites.

Materials	Current Density (A g <sup>-1</sup> )	Specific Capacity (mAh g <sup>-1</sup> )	Cycling Performance	Ref
Sb <sub>2</sub> S <sub>3</sub> @EG <sup>s</sup> -S	1	646	120	1
Sb <sub>2</sub> S <sub>3</sub> -carbon fibers	0.2	606	150	2
S-rGO/Sb <sub>2</sub> S <sub>3</sub> composite	0.5	431	600	3
Sb <sub>2</sub> S <sub>3</sub> hollow microspheres	1	656	100	4
Sb@N-C nanocomposite	0.2	603	300	5
CPC/Sb <sub>2</sub> S <sub>3</sub>	0.1	1100	200	6
	1	500	300	
Sb <sub>2</sub> S <sub>3</sub> -graphite	0.2	638	250	7
	1	496	500	
Sb <sub>2</sub> S <sub>3</sub> /graphene	0.2	670	200	8
Sb <sub>2</sub> S <sub>3</sub> @C	0.1	745	160	9
Sb <sub>2</sub> S <sub>3</sub> /MMCN@ppy	1	556	300	10
Sb <sub>2</sub> S <sub>3</sub> /CNT	0.2	443	100	11
<b>CNN@Sb<sub>2</sub>S<sub>3</sub></b>	<b>0.2</b>	<b>1056.6</b>	<b>100</b>	<b>This Work</b>
	<b>1</b>	<b>710.5</b>	<b>1500</b>	
	<b>5</b>	<b>316</b>	<b>1700</b>	
	<b>10</b>	<b>201.5</b>	<b>1000</b>	

**Table S2** Lattice constants of  $\text{Sb}_2\text{S}_3$  before cycling and after 500 cycles at  $1 \text{ A g}^{-1}$ .

Lattice constants	Before cycling ( $\text{\AA}$ )	After 500 cycles ( $\text{\AA}$ )
<i>a</i>	11.1465	10.1212
<i>b</i>	11.2618	11.1037
<i>c</i>	3.7628	4.0201

## References

- [1] S.H. Wang, Y. Cheng, H.J. Xue, W.Q. Liu, Z. Yi, L.M. Chang, L.M. Wang, Multifunctional sulfur-mediated strategy enabling fast-charging  $\text{Sb}_2\text{S}_3$  micro-package anode for lithium-ion storage, *J. Mater. Chem. A* 2021, 9, 7838-7847.
- [2] H. Yin, K.S. Hui, X. Zhao, S.L. Mei, X.W. Lv, K.N. Hui, J. Chen, Eco-friendly synthesis of self-supported N-doped  $\text{Sb}_2\text{S}_3$ -carbon fibers with high atom utilization and zero discharge for commercial full lithium-ion batteries, *ACS Appl. Energy Mater.* 2020, 3, 6897-6906.
- [3] X.Z. Zhou, Z.F. Zhang, P.F. Yan, Y.Y. Jiang, H.Y. Wang, Y.G. Tang, Sulfur-doped reduced graphene oxide/ $\text{Sb}_2\text{S}_3$  composite for superior lithium and sodium storage, *Mater. Chem. Phys.* 2020, 244, 122661.
- [4] J.J. Xie, L. Liu, J. Xia, Y. Zhang, M. Li, Y. Ouyang, S. Nie, X.Y. Wang, Template-free synthesis of  $\text{Sb}_2\text{S}_3$  hollow microspheres as anode materials for lithium-ion and sodium-ion batteries, *Nano-micro Lett.* 2018, 10, 12.
- [5] W. Luo, F. Li, J.J. Gaumet, P. Magri, S. Diliberto, L. Zhou, L.Q. Mai, Bottom-up confined synthesis of nanorod-in-nanotube structured  $\text{Sb}@N\text{-C}$  for durable lithium and sodium storage, *Adv. Energy Mater.* 2018, 8, 1703237.
- [6] V. Mullaivananathan, N. Kalaiselvi.  $\text{Sb}_2\text{S}_3$  added bio-carbon: Demonstration of potential anode in lithium and sodium-ion batteries, *Carbon* 2019, 144, 772-780.
- [7] Y.X. Liu, Z.C. Lu, J. Cui, H. Liu, J. Liu, R.Z. Hu, M. Zhu, Plasma milling modified  $\text{Sb}_2\text{S}_3$ -graphite nanocomposite as a highly reversible alloying-conversion anode material for lithium storage, *Electrochim. Acta* 2019, 310, 26-37.
- [8] Y.C. Dong, S.L. Yang, Z.Y. Zhang, J.-M. Lee, J.A. Zapien, Enhanced electrochemical

performance of lithium ion batteries using  $\text{Sb}_2\text{S}_3$  nanorods wrapped in graphene nanosheets as anode materials, *Nanoscale* 2018, 10, 3159-3165.

[9] W. Luo, X. Ao, Z.S. Li, L. Lv, J.G. Li, G. Hong, Q.H. Wu, C.D. Wang, Imbedding ultrafine  $\text{Sb}_2\text{S}_3$  nanoparticles in mesoporous carbon sphere for high-performance lithium-ion battery, *Electrochim. Acta* 2018, 290, 185-192.

[10] W.H. Yin, W.W. Chai, K. Wang, W.K. Ye, Y.C. Rui, B.H.J. Tang, A highly Meso@Microporous carbon-supported antimony sulfide nanoparticles coated by conductive polymer for high-performance lithium and sodium ion batteries, *Electrochim. Acta* 2019, 321, 134699.

[11] I. Elizabeth, B.P. Singh, S. Gopukumar, Electrochemical performance of  $\text{Sb}_2\text{S}_3/\text{CNT}$  free-standing flexible anode for Li-ion batteries, *J. Mater. Sci.* 2019, 54, 7110-7118.